CONF-960639--2

Calculations of Radiation Damage in Target, Container and Window Materials for Spallation Neutron Sources

M. S. Wechsler*, P. D. Ferguson^, L. K. Mansur#, and W. F. Sommer^
*North Carolina State University, Dept. of Nuclear Engineering, Raleigh, NC 27695-7909
^Mail Stop H805, Los Alamos National Laboratory, Los Alamos, NM 87545
#Mail Stop 6376, Oak Ridge National Laboratory, Oak Ridge, TN 37831-6376

Radiation damage in target, container, and window materials for spallation neutron sources is an important factor in the design of target stations for accelerator-driver transmutation technologies. Calculations are described that use the LAHET and SPECTER codes to obtain displacement and helium production rates in tungsten, 316 stainless steel, and Inconel 718, which are major target, container, and window materials, respectively. Results are compared for the three materials, based on neutron spectra for NSNS and ATW spallation neutron sources, where the neutron fluxes are normalized to give the same flux of neutrons of all energies.

Spallation neutron sources (SNS's) have a number of applications. These include sources for neutron scattering research facilities, accelerator production of tritium (APT), and accelerator transmutation of nuclear waste (ATW). Four SNS's are presently operating: ISIS, LANSCE, IPNS, and KENS. The highest operating beam power, at ISIS, is only 160 kW. But, a number of higher-powered SNS's are in various stages of development, ranging from slightly under 1 Mw for SINQ to 5Mw for ESS [1].

Spallation occurs when the energy of a bombarding projectile particle (usually, a proton) is sufficiently high so that, when it impinges on the target nucleus, it is able to interact separately with individual nucleons. An internuclear collision cascade is then set in motion, resulting in the emission of high energy particles, chiefly neutrons. Furthermore, the struck nucleus is left in an excited state, and it relieves this excitation energy by processes of fission or evaporation of further particles. As a rough criterion for the energy of incident proton above which spallation may occur, we may set $\lambda = R$, where λ is the deBroglie wavelength and R is the nuclear radius. This minimum energy for spallation can be shown to be approximately 10-20 MeV for tungsten and 20-50 MeV for Cr, Fe, and Ni [2]. In fact, in order to maximize the neutron yield, the proton energies anticipated for the 1-5 Mw SNS's under design are in the 1000-1600 MeV range, and the resultant neutron energy spectra extend up to these energies as well. As has been pointed out [3-4], based on an extensive literature on the effects of fission reactor irradiations at lower energies (average neutron energy of only 1-2 MeV), it is clear that materials can be severely damaged in proton and neutron environments at the SNS energies.

The purpose of the present paper is to make preliminary calculational estimates of spallation radiation damage in terms of the production of displacements and helium. The materials chosen for study are tungsten (a primary target material, now used in the LANSCE SNS), 316 stainless steel (a prime candidate container material), and Inconel 718 (now in use as beamline window at the LAMPF accelerator). The compositions chosen for 316 stainless steel and Inconel 718 are Fe-18%Cr-10%Ni and Ni-18.5%Cr-18.5%Fe-5.1%Nb-3%Mo (all wt percents), respectively. The computer codes used in this investigation are LAHET [5] and SPECTER [6] for the calculation of displacement and helium production cross sections and MCNP [7] for the calculation of spallation neutron flux and spectrum. Further details of the calculation of the cross sections are given in [8-10].

For calculation of radiation damage in the spallation neutron environment, we first obtain the differential displacement or helium production rate as a function of neutron energy by

*Research sponsored by the Division of Materials Sciences, U.S. Department of Energy under contract number DE-AC05-96OR22464 with Lockheed Martin Energy Research Corporation.

multiplying the cross section for a given energy bin by the corresponding differential neutron flux. These differential rates are then integrated up to energy E to give the displacement or helium generation rate due to neutrons of energies up to E. For the damage rate due to the incident protons of energy E, the cross section at that energy is simply multiplied by the proton flux. In the present work, we are not attempting to evaluate the damage due to the spectrum of secondary protons, but prior work has indicated that this is a small fractions of the damage due to the primary protons.

In what follows, we wish to compare displacement and helium production in tungsten, 316 stainless steel, and Inconel 718 based on using two particular SNS neutron spectra. The first neutron spectrum stems from a simplified ATW target and blanket system, consisting of a homogeneous mixture of tungsten and water (0.25 m radius; 85% volume fraction occupied by the tungsten) surrounded by heavy water [10]. The proton flux of 1600 MeV protons (flat beam, 20 cm radius) incident on the target is taken here to be 4×10^{14} protons/cm^{2}s, corresponding to a current density of about 64 μA/cm^2. By comparison, the maximum current density projected for ESS is 200 μA/cm^2 [1]. The total neutron flux of all energies corresponding to the ATW proton flux of 4×10^{14} p/cm^{2}s at the edge of the target is $\phi(\text{tot}) = 4.2 \times 10^{15}$ n/cm^{2}s. The second neutron spectrum is that of the National Spallation Neutron Source, NSNS (formerly ORSNS), which uses 1200 MeV protons and a liquid Hg target. The protons are incident on a 316 stainless steel first-wall nose cone. The two neutron spectra are shown in FIG. 1, along with the prompt neutron fission spectrum. The

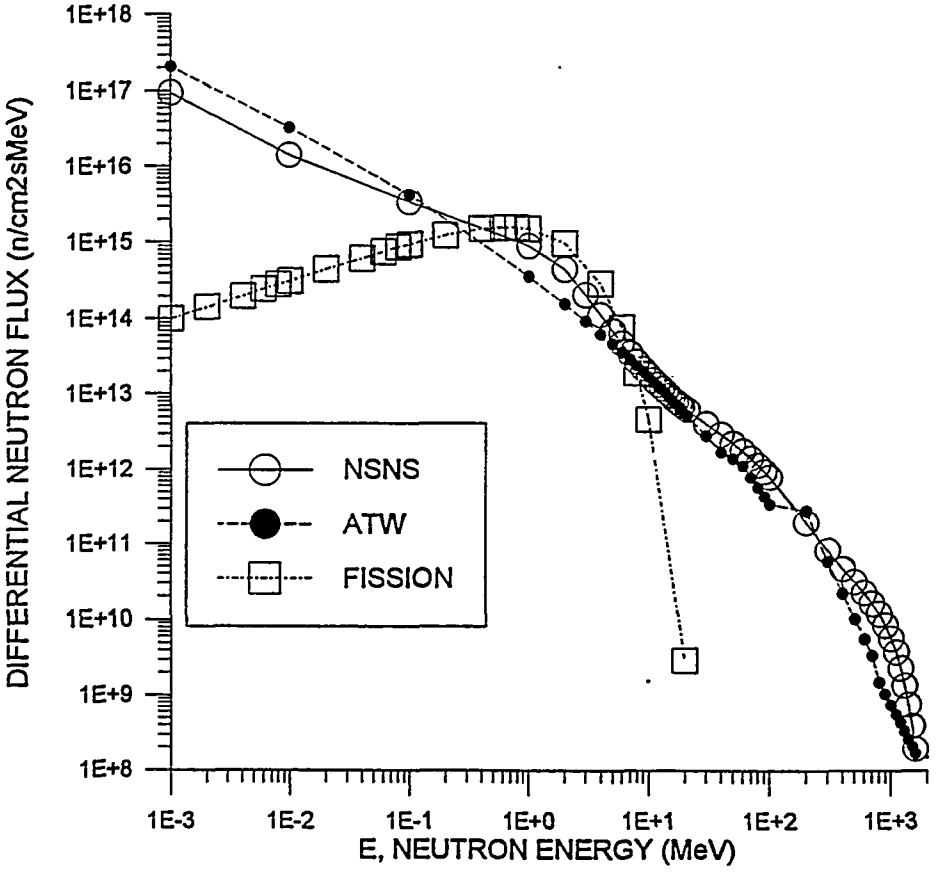

FIG. 1. Neutron spectra that we used for NSNS and ATW, and the prompt fission spectrum for comparison, all normalized to $\phi(\text{tot}) = 4.2 \times 10^{15}$ n/cm^{2}s.

spectrum for NSNS has the same shape as the one calculated for the actual system in its present design [11], but to facilitate comparison with ATW we have taken ϕ(tot) to have the same value of 4.2 x 10^{15} n/cm^{2}s as for the ATW spectrum. In fact, the present estimate is that the ϕ(tot) more likely to be about 2E14 n/cm^{2}s at the first-wall nose cone and the incident proton flux about 3 x 10^{13} p/cm^{2}s [11].

RESULTS

The displacement cross sections for W, 316 stainless steel, and Inconel are shown in FIG. 2. The calculations for E < 20 MeV were done using SPECTER and for E > 20 MeV using LAHET. At 20 MeV there is a discrepancy that seems to increase with decreasing mass of the target nucleus, but for the three materials under investigation here is not likely to be a large factor. We see that the displacement cross section for tungsten rises above that of the other two materials at high neutron energies, but falls below the other two at lower energies. As is seen below, because of the higher differential neutron fluxes at lower energies, the total displacement rate is greater for the two alloys than for W. The somewhat irregular displacement cross sections at the lowest neutron energies are due to (n,γ) events, in which the nucleus absorbs a neutron and emits a capture gamma ray, whereupon the nucleus recoils to conserve momentum. As is seen below, this process does not appear to make a significant contribution to the overall displacement production rate.

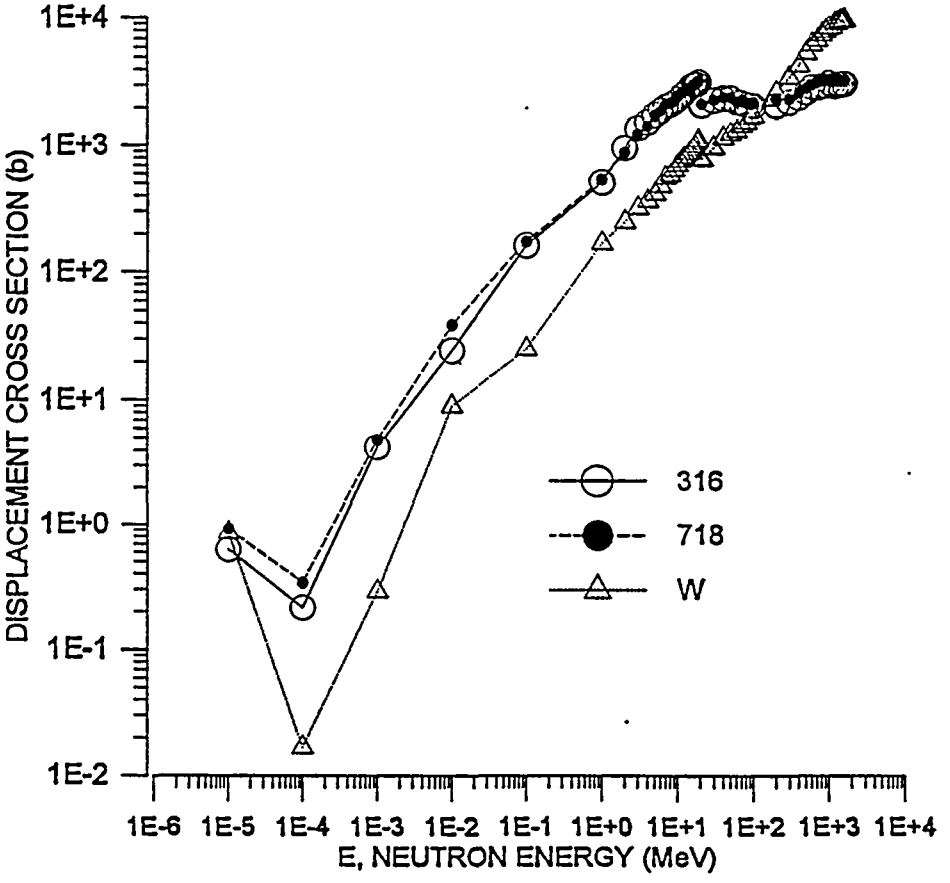

FIG. 2. Displacement cross section vs neutron energy for W, 316 stainless steel, and Inconel 718 as calculated by SPECTER (E < 20 MeV) and LAHET (E > 20 MeV).

When the displacement cross sections in FIG. 2 are folded into the differential neutron fluxes for NSNS and ATW, the result gives the differential displacement rate, and when this is integrated from the lowest energies to energy E, the result is the displacement rate due to neutrons of energies below E, as shown in FIG. 3. We note that the displacement production rate does not begin to rise appreciably until the energy increases to about 0.1 MeV. Also, the displacement rates for 316 stainless steel and Inconel 718 are almost the same for each spectrum, but greater for NSNS than for ATW. The displacement rates for W are lower than for 316 stainless steel and Inconel 718, as mentioned above, because of the greater differential neutron fluxes at lower energies where the displacement cross sections for the two alloys are greater than those for W (FIGS 1 and 2). The total displacement rates for all neutron energies, K_d, are given in TABLE 1, where we see that the K_d's for the normalized NSNS are about 60% greater than those for ATW. Also, we see that the fraction of displacements due to neutrons of energies above 20 MeV is only about 20 % for the alloys and 42 % for W. The median energy, for which equal numbers of displacements are due to neutrons of energy above and below this energy, is about 3-5 MeV for the alloys and about 10-13 MeV for W.

The displacement rates due to the incident proton beam, here taken to have a flux of 4 x 10^{14} p/cm^{2}s for both NSNS and ATW, are also shown in TABLE 1. We see that the total displacement rate is lower due to the incident protons than for the spectrum of neutrons for the two alloys for both NSNS and ATW, but the reverse is true for W.

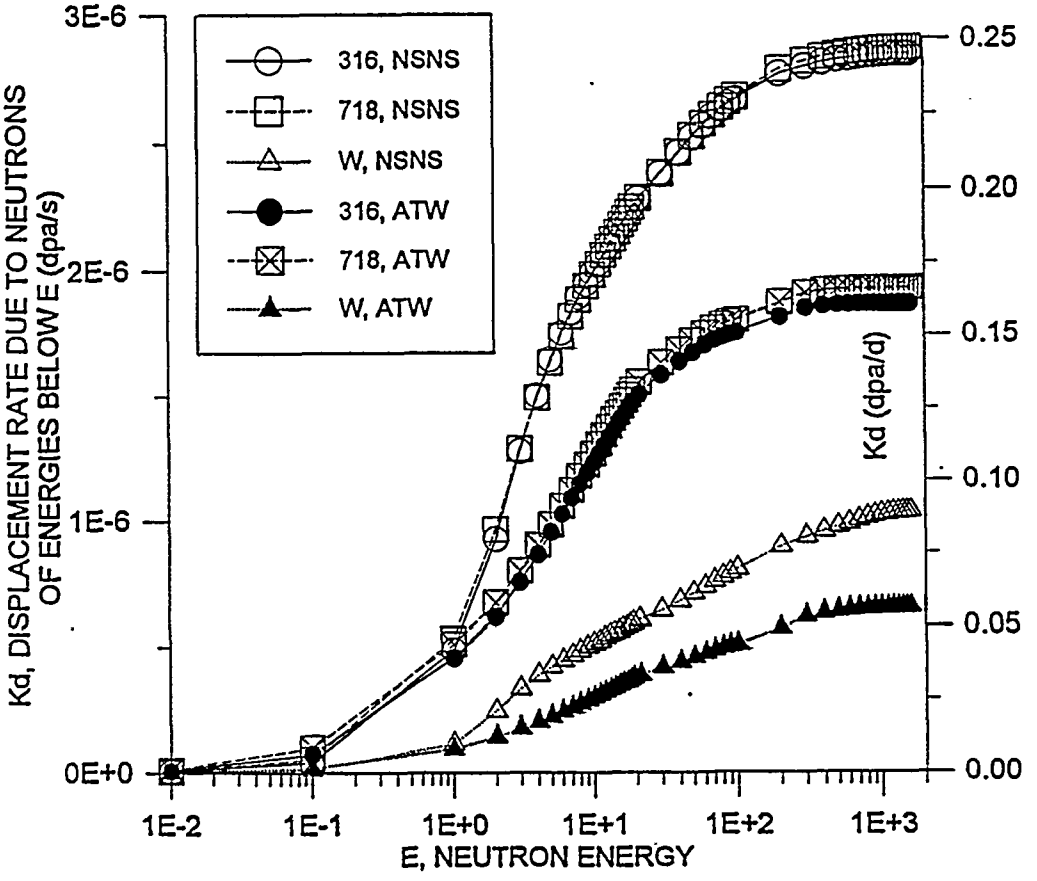

FIG. 3. Displacement production rate, K_d, due to neutrons of energies below E vs neutron energy E for W, 316 stainless steel, and Inconel 718 in NSNS and ATW neutron spectra.

Table 1. Summary of Displacement and He Production in NSNS* and ATW Spectra

	NSNS	ATW
Neutrons, ϕ(tot)=4.2E15 n/cm^{2}s)		
K_d (DPA/d)		
316	0.25	0.16
718	0.25	0.17
W	0.089	0.056
Median E (MeV)		
316	3.6	4.8
718	3.7	4.7
W	10.4	13
% due to n's of E>20 MeV		
316	20	20
718	21	20
W	42	41
K(He), (appm He/d)		
316	1.6	1.1
718	2.7	2.0
W	0.85	0.33
Median E (MeV)		
316	45	23
718	16	14
W	640	330
% due to n's of E>20 MeV		
316	62	52
718	42	33
W	100	100
Protons (ϕ=4E14 p/cm^{2}s)		
K_d (DPA/d)		
316	0.10	0.10
718	0.11	0.11
W	0.32	0.32
K(He), (appm He/d)		
316	16	16
718	17	17
W	80	80

*The proton and neutron fluxes shown for NSNS (formerly, ORSNS) are chosen in order to facilitate comparison with results for the ATW neutron spectrum. Preliminary estimates of the actual proton and neutron fluxes for NSNS are presently about 3E13 p/cm^{2}s and 2E14 n/cm^{2}s at the first-wall nose cone [11].

The helium production rates, K(He), due to spallation neutrons at NSNS and ATW are shown in FIG. 4. The K(He) for Inconel 718 are greater than for 316 stainless steel, particularly below 20 MeV and largely due to the greater (n,α) cross section for Ni than for Cr and Fe. In addition, He production is greater in NSNS than in ATW. Furthermore, we

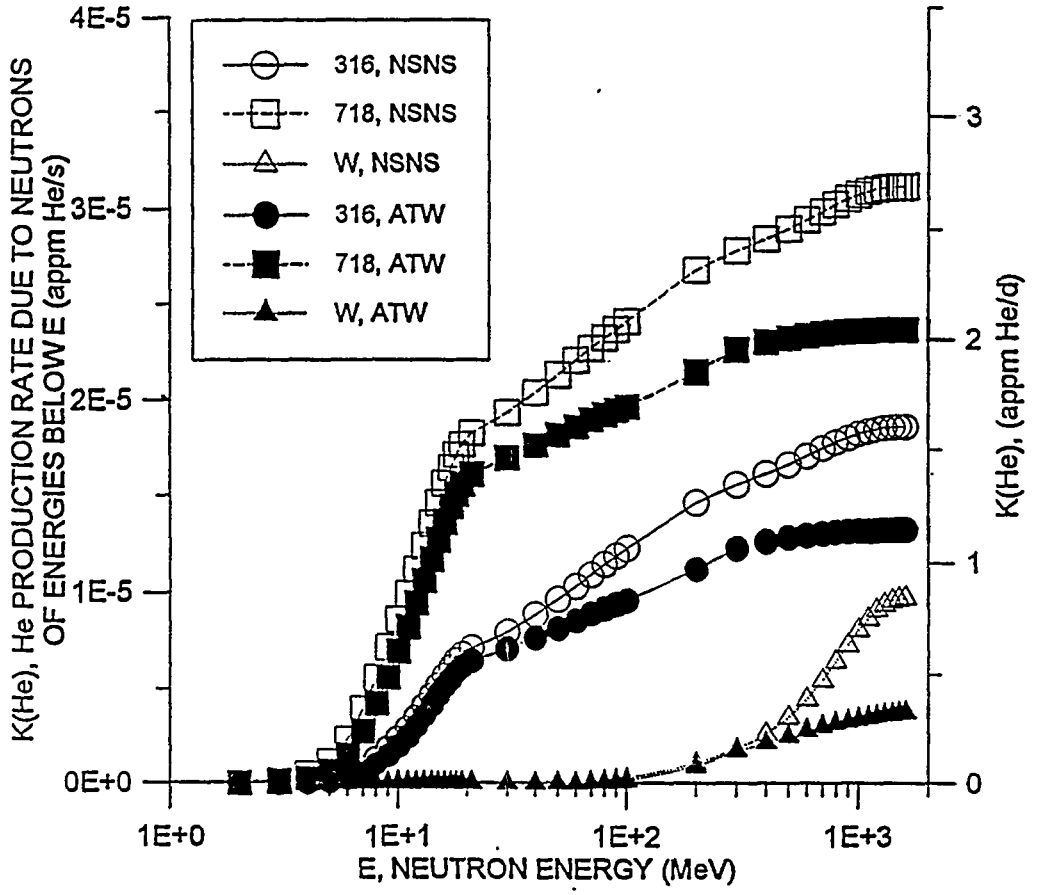

FIG. 4, Helium production rates, K(He), due to neutrons of energies below E vs neutron energy E for W, 316 stainless steel, and Inconel 718 in NSNS and ATW neutron spectra.

see in FIG. 4 that the production of He is greater in the two alloys than in W. He production does take a spurt upward for W in NSNS spectrum above that for the ATW spectrum at energies above about 500 MeV. This is because the He production cross section increases strongly above a few hundred MeV, and the NSNS neutron flux is greater there than for ATW (FIG. 1). The total He production rates for the three materials and the two neutron spectra are shown for neutron and proton irradiations in TABLE 1.

DISCUSSION

The discrepancy between the displacement cross sections at 20 MeV as obtained from LAHET and SPECTER calculations, as shown in FIG. 2 is a matter that is presently under investigation. As mentioned above, the discrepancy seems to increase with decreasing mass of the bombarded material. Since the nucleus radius decreases with decreasing mass, it becomes more difficult to meet the criterion that the deBroglie wavelength be shorter than the nuclear radius, and the conditions such that the intranuclear cascade model inherent in the LAHET code be valid require higher energies of the incident projectile (neutron or proton). Another factor under consideration is that the LAHET code does not follow neutrons of energies below a cutoff energy usually set at 20 MeV. Neutrons emerging from a reaction with energy below 20 MeV have their kinematical parameters stored in a file

called NEUTP, and we are investigating the possibility of using the information in this file in order to see whether displacements due to these below-20-MeV neutrons might help to reduce the discrepancy.

The displacement production rates displayed in TABLE 2 have, in any case, the potential for causing significant deterioration in material properties. For example, Garner [12] states that exposures of 1-10 DPA cause rapid decreases in fracture toughness, and he presents a figure to support the statement for steels including 316 stainless steel and Inconel 600 and 800. TABLE 1 indicates displacements rates of about 0.2 DPA/d for 316 stainless steel and Inconel 600, so that 1-10 DPA would be reached in 2-20 days. (However, the figure in [12], on page 528, refers to irradiations and tests at 400 ^{o}C, which is somewhat above expected exposure temperatures in SNS's).

The effects of irradiation-produced helium are also a matter of some concern. The calculated helium generation rates, particularly for the proton irradiation case, are exceedingly high.

REFERENCES

[1] Bauer, G, Atchison, F., Broome, T. A. and Conrad, H. M, "A Target Development Program for Beamhole Spallation Neutron Sources in the Megawatt Range", in AIP Conference Proceedings 346, International Conference on Accelerator-Driven Transmutation Technologies and Applications, American Institute of Physics, Woodbury, NY, 1995, pp. 105-116.

[2] Wechsler, M. S., Lin, C., Sommer, W. F., Daemen, L. L., and Ferguson, P. D., "Radiation Effects in Materials for Accelerator-Driven Neutron Technologies", submitted for the Proceedings of the Symposium on Radiation Materials Science in Technology Applications, Anaheim, California, February 4-8, 1996. To be published in J. Nucl. Mater.

[3] Stubbins, J. F., Wechsler, M. S., Borden, M., and Sommer, W. F., "Behavior of Structural and Target Materials Irradiated in Spallation Neutron Environments", in AIP Conference Proceedings 346, International Conference on Accelerator-Driven Transmutation Technologies and Applications, American Institute of Physics, Woodbury, NY, 1995, pp. 879-888.

[4] Wechsler, M. S., Stubbins, J. F., Sommer, W. F., Ferguson, P. D., and Farnum, E. H., "Selection and Qualification of Materials for the Accelerator Transmutation of Waste Project", LA-UR-92-1211, Los Alamos National Laboratory, Los Alamos, NM, 1992.

[5] Prael, R. E., and Lichtenstein, H. "User Guide to LCS: The LAHET Code System," Los Alamos National Laboratory Report LA-UR 89-3014, 1989.

[6] Greenwood, L. R. and Smither, R. K., "SPECTER: Neutron Damage Calculations for Materials Irradiations", Argonne National Laboratory Report ANL/FPP/TM-197, 1985.

[7] Briesmeister, J. F. Editor, "MCNP--A General Monte Carlo Code for Neutron and Photon Transport", Version 3A, Los Alamos National Laboratory Report LA-7396-M, Rev. 2, 1986.

[8] Wechsler, M. S., Lin, C., and Sommer, W. F., "Basic Aspects of Spallation Radiation Damage to Materials", in AIP Conference Proceedings 346, International Conference on Accelerator-Driven Transmutation Technologies and Applications, American Institute of Physics, Woodbury, New York, 1995, pp. 466-475.

[9] Wechsler, M. S., Ramavarapu, R., Daugherty, E. L., Palmer, R. C., Bullen, D. B., and Sommer, W. F., "Calculation of Displacement, Gas, and Transmutation Production in Stainless Steel Irradiated with Spallation Neutrons", J. Nucl. Matls, Vols. 212-215, pp. 1678-1681, 1994.

[10] Wechsler, M. S., Ferguson, P. D., Lin, C., and Sommer, W. F., Spallation Radiation Damage and Dosimetry for Accelerator Transmutation of Waste Applications, pp. 782-791 in Reactor Dosimetry, STP 1228, edited by H. Farrar, E. P. Lippincott, J. G. Williams, and D. W. Vehar, American Society for Testing and Materials, Philadelphia, 1994.

[11] Private communication, J. J. Johnson, L. A. Charlton, and J. M. Barnes, Oak Ridge National Laboratory.

[12] Garner, F. A., "Irradiation Performance of Cladding and Structural Steels in Liquid Metal Reactors", Nuclear Materials and Technology, Chapter 6, Volume 10A-Nuclear Materials, 1994, pp. 419-543.

DISCLAIMER